Ablation of Pyrophosphate Regulators Promotes Periodontal Regeneration

Atsuhiro Nagasaki[1], Karin Nagasaki[1], Emily Y. Chu[1], Bernice D. Kear[1], Wongelawit D. Tadesse[1], Shelby E. Ferebee[1], Brian L. Foster[4], Martha J. Somerman[1]

1. Laboratory of Oral Connective Tissue Biology, National Institute of Arthritis and Musculoskeletal and Skin Diseases (NIAMS), National Institutes of Health (NIH), Bethesda, MD, USA

2. Biosciences Division, College of Dentistry, The Ohio State University, Columbus, OH, USA

Corresponding author:

Dr. Atsuhiro Nagasaki

Laboratory of Oral Connective Tissue Biology,

National Institute of Arthritis and Musculoskeletal and Skin Diseases (NIAMS),

National Institutes of Health (NIH)

9000 Rockville Pike, Building 50, Room 4120

Bethesda, Maryland, 20892

Tel: 301-594-0588

email: atsuhiro.nagasaki@nih.gov

APPENDIX MATERIALS AND METHODS

Mandibular Fenestration Defects

We used a modified fenestration root surface defect model in mice (Appendix Figure 1A) (King et al. 1997; Rodrigues et al. 2011). Surgeries were performed on 5-week-old mice. Mice were anesthetized by intraperitoneal administration of 100 mg/kg ketamine and 7 mg/kg xylazine. Incisions were made along buccal skin and muscles and tissues were separated conservatively. A periodontal fenestration bone defect (approximately 2 mm x 1 mm) was created on the buccal aspect of left mandibular bone around the distal root of first molar and mesial root of the second molar. Acellular cementum and superficial dentin were removed using a 2 mm round dental bur with saline irrigation. Surrounding muscles and skin were repositioned, and the skin incision was closed with 4-0 Coated VICRYL (Polyglactin 910), (Ethicon Inc., Somerville, NJ, USA). Buprenorphine (0.05 mg/20 g) was given subcutaneously at once before or after surgery for pain control and a second does was administered to mice when mice exhibited distress. In addition to normal diet, a soft diet gel (Diet Gel 31M, ClearH2O, Portland, ME) was provided post-surgery until mice were euthanized at postoperative day (POD) 15 or 30. All surgical wounds healed well. There were no signs of infection, neither skin nor oral mucosa invaded the defect area, and all mice continued to feed and gain weight normally. Mandibles were harvested for analysis at POD 15 and 30 (n=4 mice/genotype at POD15 and 30 for microCT and histology; n=3-4 mice/genotype at POD30 for double fluorochrome labeling). Male and female mice were combined because no significant sex-related differences in cementum or alveolar bone were noted in a previous study (Chu et al. 2020).

Micro-computed Tomography (microCT)

Mandibles were fixed in 10% neutral buffered formalin for 48 hours at room temperature prior to microCT scanning. To measure volume and mineral density of regenerated alveolar bone, microCT analysis was performed using methods modified from a previous study (Ao et al. 2017).

A standard curve was calculated using 5 hydroxyapatite (HA) standards of known densities (mg HA/cm^3). To limit analysis to the local area of regenerated bone, a region of interest was created beginning at the center between the mandibular first molar mesial and distal roots and extending 150 slices mesiodistally (900 µm) and 120 axial slices (720 µm) from the root apex. Bone and partially mineralized osteoid volumes were identified by anatomical location and thresholds of 650 mg HA/cm^3 and 360 mg HA/cm^3, respectively.

Histology

Formalin fixed mandibles were demineralized in an acetic acid/formalin/sodium chloride (AFS) solution for 4 weeks, stored in 70% ethanol, and processed for standard paraffin embedding. Because the defect was limited in size, 20-30 serial sections were prepared from each sample. To standardize the approach, we used the same axial level slide for each staining, i.e., we matched histological section numbers between samples for each analysis, e.g. slide #1 from each sample was stained by hematoxylin and eosin (H&E), slide #2 from each sample was used for immunohistochemistry, and so forth. H&E staining, immunohistochemistry (IHC), *in situ* hybridization (ISH), and tartrate-resistant acid phosphatase (TRAP) staining were performed for morphological analysis. All histological analyses were performed at the same time, and image acquisition was acquired with the same parameters at the same time.

Immunohistochemistry (IHC)

IHC was performed using a peroxidase-based kit (Vector Laboratories, Inc., Burlingame, CA) with a 3-amino-9-ethylcarbazole (AEC) substrate to produce a red signal, as previously described (Ao et al. 2017; Foster et al. 2018). Primary antibodies were used with the following dilutions: 1:600 M176 polyclonal rabbit Anti-Dentin Matrix Protein1 (DMP1; Takara Bio Inc, Kusatsu, Shiga, Japan); 1:200 LF-175 polyclonal rabbit anti-mouse osteopontin (OPN; Kerafast, Inc., Boston, MA); 1:200 polyclonal rabbit anti-mouse bone sialoprotein (BSP; kindly provided by Dr. Renny

Franceschi, University of Michigan, Ann Arbor, MI); 1:200 goat polyclonal to cathepsin K (ab19027; Abcam Inc, Cambridge, MA).

In situ Hybridization (ISH)

RNAscope® H_20_2 & Protease Plus Reagents, RNAscope® 2.5 HD Detection Reagents-RED RNAscope® Probes for *Dmp1*, *Spp1* and *Ibsp* were used following manufacturer's directions (Advanced Cell Diagnostics, Newark, CA) as previously described (Foster et al. 2018). To measure ISH staining positive area, photographs of regenerated cementum were cropped to 60 pixels X 300 pixels using Adobe Photoshop (Adobe Inc., San Jose, CA) and alveolar bone images were captured in each section under 200X magnification. Color images were converted to binary (black/white) images and then positive (black) pixels were counted with ImageJ software (Version 1.53a) (Bethesda, MD).

Tartrate-Resistant Acid Phosphatase (TRAP) Staining

A TRAP/alkaline phosphatase (ALP) stain Kit was used following manufacturer's directions (Wako Pure Chemical Industries, Ltd., Osaka, Japan).

Double fluorochrome labeling

For dynamic measurements of cementum and bone regeneration, calcein and alizarin red mineralized tissue fluorochromes were employed using a modification of a previously described method (Rodrigues et al. 2011). Mice were given an intraperitoneal (IP) injection of 12.5 mg/kg calcein (Sigma-Aldrich, St. Louis, MO) on POD7. On POD14, mice were given an IP injection of 30 mg/kg alizarin red (Electron Microscopy Sciences, Hatfield, PA). Mice (n=3-4 mice/genotype) were sacrificed on POD30. Mandibles were collected and fixed in 70% ethanol for 48 hours, dehydrated in a graded ethanol series, and embedded in methyl methacrylate. Samples were cut

into transverse 6 µm sections and unstained sections were viewed under an epifluorescence illumination microscope.

APPENDIX FIGURES

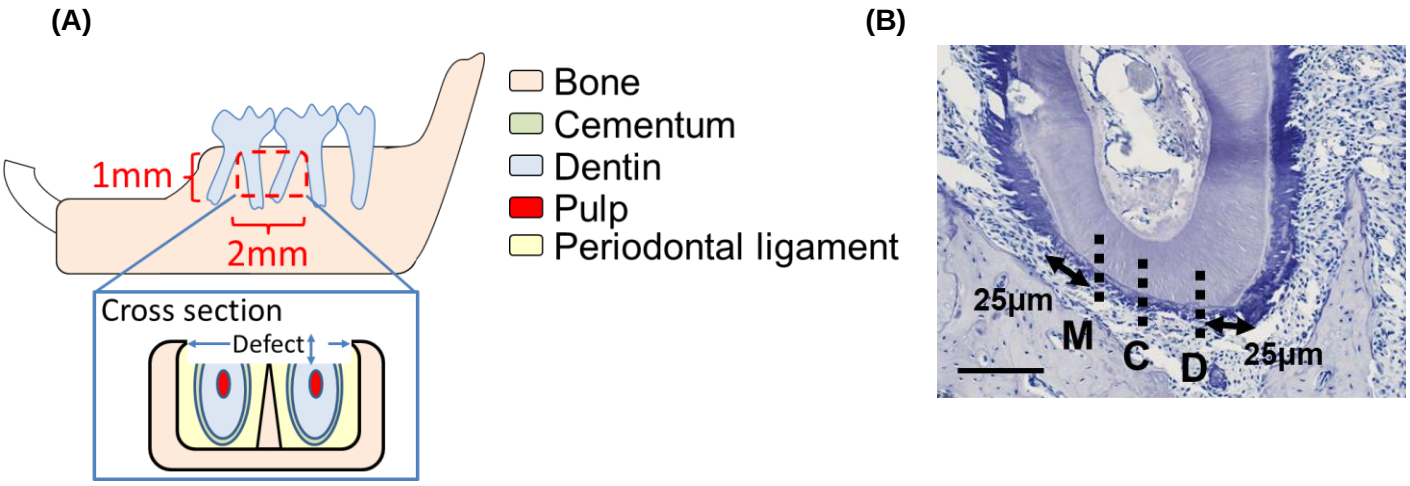

Appendix Figure 1. Creation of the Periodontal Fenestration Defect and Measurement of Cementum Regeneration. (A) Periodontal fenestration defects (approximately 2 mm x 1 mm) were created by removal of alveolar bone, cementum, and superficial dentin on the buccal aspect of the distal root of mandibular first molar and mesial root of the second mandibular molar. **(B)** Regenerated cementum thickness was measured in transverse histological sections at 3 points: mesial (M), central (C), and distal (D) locations within the fenestration defects. Mesial and distal points were determined at 25 μm from the respective edges of the defect. Scale bar: 50 μm.

(A)

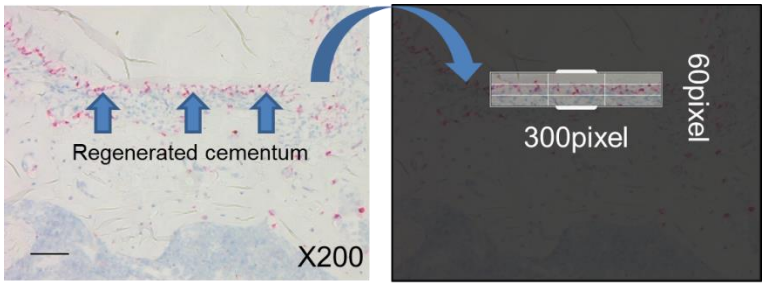
Regenerated cementum
X200
60pixel
300pixel

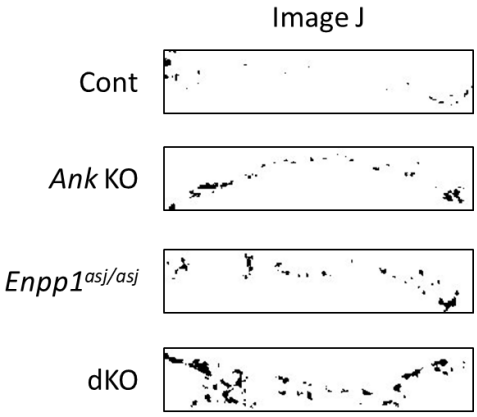
Image J
Cont
Ank KO
Enpp1asj/asj
dKO

(B)

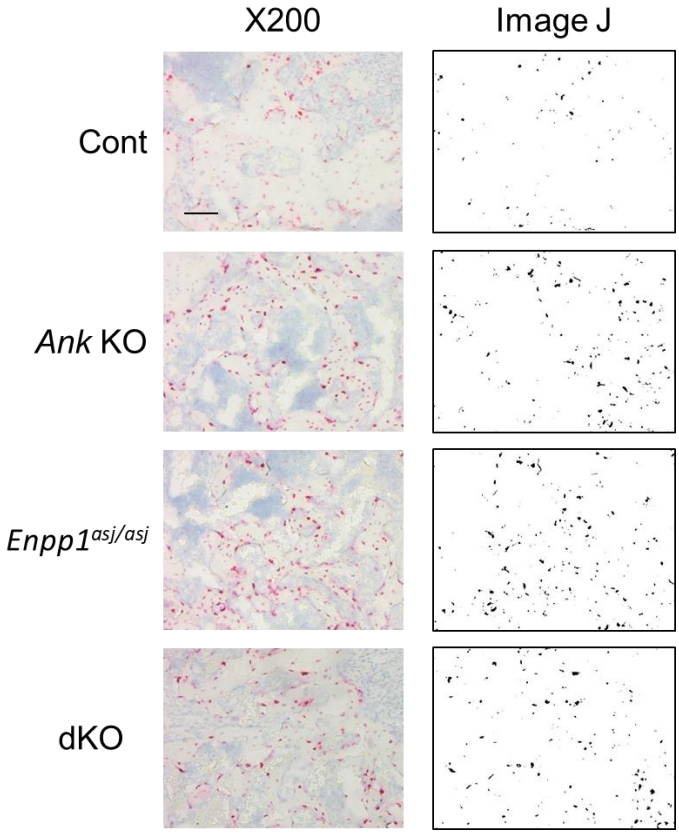
X200
Image J
Cont
Ank KO
Enpp1asj/asj
dKO

Appendix Figure 2. Quantitative Analysis of ISH Staining. (A) To provide a quantitative measure of target gene expression by ISH, photomicrographs of regenerated cementum surfaces were taken under 200X magnification and cropped to 60 pixels X 300 pixels using Adobe Photoshop, to specifically select only the region of regenerated cementum and immediately adjacent cells. Cropped images were imported into ImageJ software and binary (black/white) images were created. Positive (black) areas were measured with ImageJ software (Version 1.53a) (Bethesda, MD). **(B)** Alveolar bone image of buccal side of the distal root of the first molar was photographed for each section under 200X magnification and analyzed in ImageJ as well as regenerated cementum. Scale bar: 50 μm.

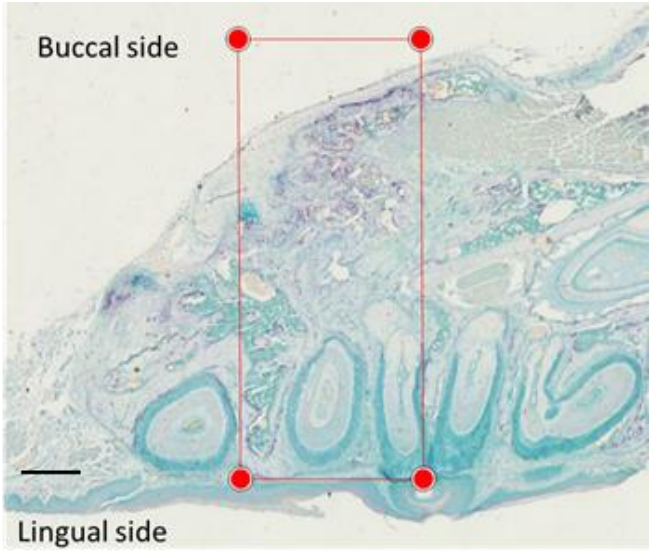

Appendix Figure 3. Osteoclast Counts in Regenerated Alveolar Bone. Tartrate-resistant acid phosphatase (TRAP) staining and IHC for cathepsin K was performed to analyze the effects from *Ank* and/or *Enpp1* ablation on osteoclastogenesis in regenerated alveolar bone. The numbers of $TRAP^+$ or cathepsin K^+ cells, multinucleated, osteoclasts, were counted in regenerated alveolar bone (representative image: TRAP staining, inside the square: from interradicular septa of the first molar to interradicular septa of the second molar). Scale bar: 200 μm.

REFERENCES

Ao M, Chavez MB, Chu EY, Hemstreet KC, Yin Y, Yadav MC, Millan JL, Fisher LW, Goldberg HA, Somerman MJ et al. 2017. Overlapping functions of bone sialoprotein and pyrophosphate regulators in directing cementogenesis. Bone. 105:134-147.

Foster BL, Ao M, Salmon CR, Chavez MB, Kolli TN, Tran AB, Chu EY, Kantovitz KR, Yadav M, Narisawa S et al. 2018. Osteopontin regulates dentin and alveolar bone development and mineralization. Bone. 107:196-207.

King GN, King N, Cruchley AT, Wozney JM, Hughes FJ. 1997. Recombinant human bone morphogenetic protein-2 promotes wound healing in rat periodontal fenestration defects. J Dent Res. 76(8):1460-1470.

Rodrigues TL, Nagatomo KJ, Foster BL, Nociti FH, Somerman MJ. 2011. Modulation of phosphate/pyrophosphate metabolism to regenerate the periodontium: A novel in vivo approach. J Periodontol. 82(12):1757-1766.